ACS APPLIED NANO MATERIALS
Cite This: ACS Appl. Nano Mater. 2019, 2, 3490−3500
Article
www.acsanm.org

# Stoppers and Skins on Clay Nanotubes Help Stabilize Oil-in-Water Emulsions and Modulate the Release of Encapsulated Surfactants

Olakunle Francis Ojo,[†] Azeem Farinmade,[†] James Trout,[†] Marzhana Omarova,[†] Jibao He,[‡] Vijay John,[*,†] Diane A. Blake,[§] Yuri M. Lvov,[∥] Donghui Zhang,[⊥] Duy Nguyen,[#] and Arijit Bose[%]

[†]Department of Chemical & Biomolecular Engineering and [‡]Coordinated Instrumentation Facility, Tulane University, 6823 St. Charles Avenue, New Orleans, Louisiana 70118, United States
[§]Tulane University School of Medicine, 1430 Tulane Avenue, New Orleans, Louisiana 70118, United States
[∥]Institute for Micromanufacturing, Louisiana Tech University, 911 Hergot Avenue, Ruston, Louisiana 71272, United States
[⊥]Department of Chemistry, Louisiana State University, 207 Choppin Hall, Baton Rouge, Louisiana 70803, United States
[#]Nalco Champion, an Ecolab Company, 7705 Highway 90-A, Sugar Land, Texas 77478, United States
[%]Department of Chemical Engineering, University of Rhode Island, Kingston, Rhode Island 02881, United States

Supporting Information

**ABSTRACT:** This work develops the concepts of particle-stabilized emulsions using tubular natural clays known as halloysites to attach to the oil−water interface and stabilize oil-in-water emulsions. Such halloysite nanotubes (HNT) serve as reservoirs for surfactants and can deliver surfactants to the oil−water interface and thus lower the oil−water interfacial tension. This two-step concept of surfactant delivery and droplet stabilization by particles has significant implications to oil spill remediation. However, to deliver surfactant loaded HNTs in a water-based solvent slurry, it is important to stopper the nanotubes to prevent premature release of the surfactant. This work focuses on the use of an environmentally benign two-dimensional metal−organic framework formed by coordinating Fe(III) with a polyphenolic as a stoppering agent. Such metal−phenolic networks (MPN) form a skin around the HNTs, thus providing a way to effectively sequester surfactant cargo for controlled release. Cryo-scanning electron microscopy (Cryo-SEM) shows that these HNTs and HNT bundles attach to the oil−water interface with side-on orientation. Inverted drop tensiometry was used to characterize the dynamic interfacial tension resulting from the release of a model surfactant (Tween 80) from the HNTs and indicates that the MPN stoppers are effective in sequestering the surfactant cargo for extended periods at neutral pH values. Release triggered by MPN disassembly at acidic pH values can be performed just prior to delivery to oil spills. The concepts and scalability of this process have significant implications for oil spill remediation, enhanced oil recovery, and biomedical and pharmaceutical applications.

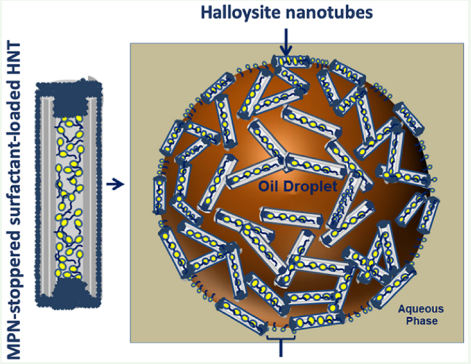


**KEYWORDS:** *halloysites, metal−phenolic network, oil spill, Pickering emulsions, stoppers*

## 1. INTRODUCTION

The Deepwater Horizon incident in 2010 has led to tremendous research efforts in oil spill remediation technologies.[1] One of the most effective techniques for the treatment of large spills is the use of dispersants which are essentially surfactant solutions dissolved in appropriate solvents such as propylene glycol and petroleum distillates. Such surfactants reduce the oil−water interfacial tension and allow the oil to break up into small emulsion droplets that become dispersed in the water column and are eventually consumed by oil-degrading bacteria.[2−4] Emulsification involves the creation of new oil−water interfaces and thus comes with a significant energy penalty. Lowering the oil−water interfacial tension typically by using dispersants (surfactants in an appropriate solvent) can reduce this penalty. Thus, over 2.1 million gallons of dispersant were utilized during the Deepwater Horizon Oil Spill.[5] The dispersant formulation uses surfactants dissolved in organic solvents such as propylene glycol and other light petroleum distillates,[2] leading to concerns about the long-term effects of using large volumes of dispersants on the ecosystem. Thus, there is a need to optimize dispersant use, reduce solvent use, and target the dispersant to the oil−water interface.[1,6−8]

An environmentally benign approach to dispersion is the use of surface-active particles to stabilize oil-in-water emulsions through the formation of steric barriers to droplet coalescence. Such particle-stabilized emulsions, also known as Pickering

Received: March 12, 2019
Accepted: May 28, 2019
Published: May 28, 2019






DOI: 10.1021/acsanm.9b00469
ACS Appl. Nano Mater. 2019, 2, 3490−3500

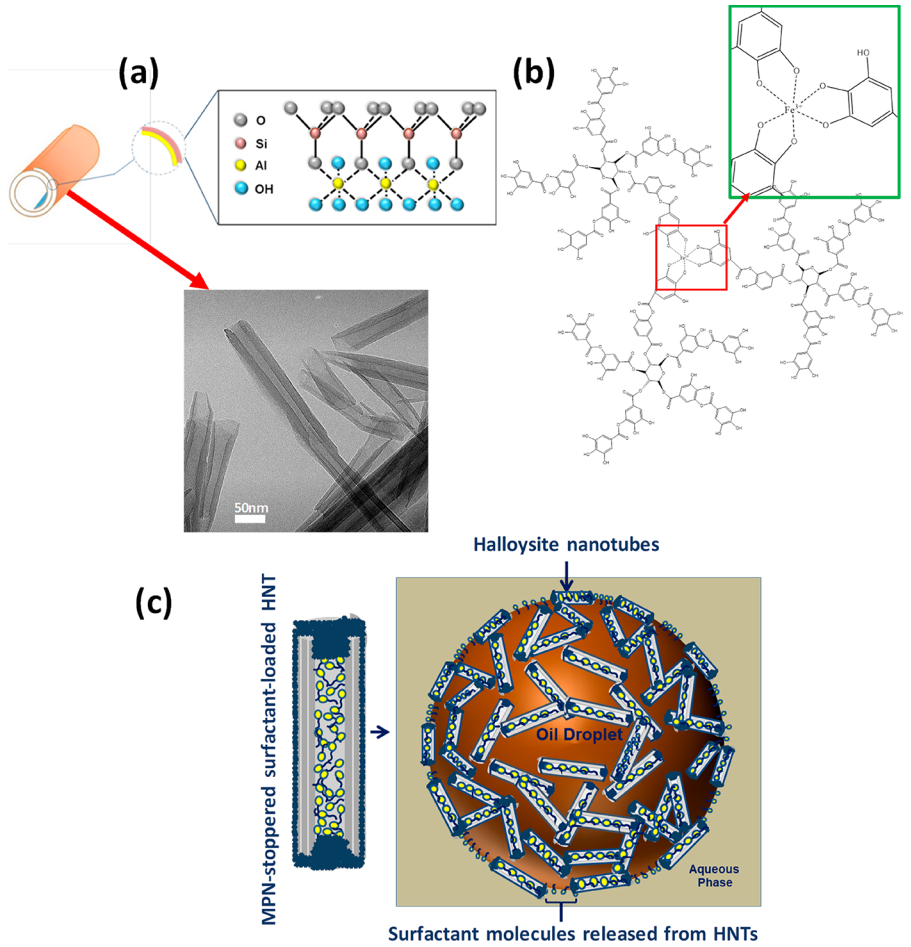


**Figure 1.** (a) Halloysite structure showing the negatively charged, Si-rich outer layer and a positively charged, Al-rich inner lumen. The characteristic dimensions of the halloysites are 1.0 $\mu$m in length with a lumen size ranging from 20 to 35 nm internal diameter. (b) Metal–phenolic network (MPN) structure formed as a result of the complexation of tannic acid molecules (as ligand) and iron (Fe) as the metallic center. (c) Schematic of interfacial network formed by MPN-stoppered halloysites containing Tween 80 at the oil–water interface.

emulsions, have been of interest since the pioneering studies of Pickering and Ramsden,[9,10] and their applications to forming stable emulsions have been studied extensively.[11−14] While particle-stabilized emulsions are highly effective in preventing coalescence, they are much less effective than surfactants in reducing the oil–water interfacial tension, especially to values of the order of $10^{-1}$ mN/m or lower required to disperse oil spills into the water column. In recent work from our laboratory, we have shown that emulsion stabilization and a reduction of interfacial tension can be implemented using natural hollow tubular nanoparticles known as halloysites that release a cargo of surfactants encapsulated within the lumen of these nanotubes.[8,14−16] Halloysite nanotubes (HNTs) are environmentally benign, widely available, naturally occurring aluminosilicates with the chemical formula $Al_2(OH)_4Si_2O_5 \cdot nH_2O$ formed by the rolling of kaolinite sheets into tubes (Figure 1a).[17] The tubular morphology of the halloysites allows them to be used as carriers for a variety of materials including pharmaceuticals anticorrosion compounds and antibacterial agents.[18−24] Figure 1a illustrates the structure of halloysite and includes a transmission electron micrograph of a halloysite nanotube clearly depicting a lumen between 25 and 40 nm in diameter.

Our specific application involves the use of halloysites to encapsulate and deliver surfactants to the oil–water interface. In our earlier work,[8,14−16,25] we were able to show that dry HNTs loaded with surfactants when dispersed into an oil and water system adsorb to the oil–water interface and quickly release their cargo to lower the interfacial tension and form extremely small droplets. The almost instantaneous delivery of surfactants is a significant drawback as it implies that HNTs must be delivered as dry materials, while traditional delivery mechanisms involve the spraying of liquid solutions onto an oil spill. Ideally, therefore it is useful to disperse the loaded HNTs in a solvent (with water preferred as a benign solvent) and prevent instantaneous release by stoppering the nanotubes. When delivered to the oil–water interface, the concept is that the halloysite will adsorb to the oil–water interface and form particle-stabilized emulsions, especially under turbulent conditions created by wave action. The objective is to allow the stoppers to then gradually break up, thus releasing surfactant which lowers the interfacial tension to create much smaller droplets that are easily dispersed in the water column. The concept of stoppering halloysites for controlled delivery has been studied in the past for applications in the delivery of encapsulated compounds. Two excellent examples are those of Abdullaev and Lvov,[23] who formed complexes with benzotriazole to slow down the release of the corrosion inhibitor, and the work of Cavallaro and co-workers,[26] who showed stoppering through the formation of $Ca_3(PO_4)_2$ to delay the



DOI: 10.1021/acsanm.9b00469
ACS Appl. Nano Mater. 2019, 2, 3490−3500

release of $Ca(OH)_2$ from within the lumen and thus control rates of deacidification upon exposure to $CO_2$.

The work described in this paper involves the use of an environmentally benign two-dimensional metal−organic framework (MOF) for coating and stoppering HNTs containing surfactant. We specifically use the metal−phenolic network (MPN) first developed through the pioneering work by Ejima and co-workers[27] where a central metal atom spontaneously coordinates to polyphenolic ligands.[28] These networks spontaneously assemble and are pH-responsive, disassembling at acidic pH values and being relatively stable at alkaline values. The concept has been exploited for developing stimuli-responsive capsules in a number of applications including drug delivery,[29−31] catalysis,[32−34] and cytoprotective coatings. Figure 1b illustrates the MPN network.

Our objective in this work is to use the unique characteristics of MPNs as stoppers for surfactant cargo loaded halloysite nanotubes for the controlled release of dispersants in oil spill remediation. We use the nonionic surfactant polyoxyethylene (20) sorbitan monooleate (Tween 80, Supporting Information S1) as a model surfactant. Tween 80 is also a component of COREXIT 9500, the dispersant used in the Deepwater Horizon incident. The work details our findings relevant to the encapsulation of Tween 80 in the lumen of HNTs, the attachment of MPN coated and stoppered HNTs containing polyoxyethylene (20) sorbitan monooleate (Tween 80) at the oil−water interface, the gradual degradation of the MPNs and release of Tween 80, and the consequent implications to the reduction of interfacial tension and oil droplet size critical for effective dispersion of oil. Aspects of this work can easily be extrapolated to other applications involving the use of halloysite as reservoirs for surfactants and other encapsulated materials.

## 2. MATERIALS AND METHODS

**2.1. Materials.** Halloysite nanotubes (HNT) were obtained through a generous gift from Professor Bing Zhang (Zhengzhou University) to Y. Lvov, sourced from mines in the Henan Province, China. The internal diameter and length of the HNTs varied between 20−35 nm and 700−1000 nm, respectively. The HNT used in this work will be provided to any researcher who wishes to obtain a sample, but the observations should be entirely valid for HNT obtained from all commercial sources; an extensive list of HNTs can be found in the paper by Pasbaksh et al.[35] Tween 80 (polyoxyethylene sorbitan monooleate, $C_{64}H_{124}O_{26}$), tannic acid ($C_{76}H_{52}O_{46}$), iron(III) chloride hexahydrate ($FeCl_3{\cdot}6H_2O$), methanol ($CH_3OH$), dodecane ($C_{12}H_{26}$), chloroform ($CHCl_3$), hydrochloric acid (HCl), buffer solutions of pH 2.0, 7.0, and 9.0, sodium chloride (NaCl), sodium hydroxide (certified ACS pellets), ammonium thiocyanate ($NH_4SCN$, ≥97.5%), and cobalt(II) nitrate hexahydrate ($Co(NO_3)_2$) were purchased from Sigma-Aldrich. The 0.6 M NaCl aqueous solution was used as a substitute for seawater. Deionized (DI) water was generated from a Millipore Direct-Q 3UV water purification system with a resistance of 18.2 MΩ and was used in all experiments. All materials were utilized as obtained without any further treatment or purification.

**2.2. Loading of Surfactant Tween 80 into Halloysite Nanotubes (HNTs).** The loading of Tween 80 into the lumen of the HNTs follows the vacuum infiltration procedure described in the literature[36] and used extensively to load cargo into the lumen including drug components, corrosion inhibitors, and surfactants.[14,25,37−40] Typically, 500 mg of HNTs was weighed into a round-bottom flask, and then a solution of 0.17 g of Tween 80 dissolved in 4 mL of methanol was added. The resulting dispersion was briefly sonicated in a batch sonicator (Cole-Parmer 8890) for 60 s to allow for even dispersion of HNT particles. The samples were then placed in a rotary evaporator, and a vacuum was applied to allow for solvent evaporation and suction of Tween 80 into the lumen of the HNTs.[41] After 15 min, the rotary evaporator was returned to atmospheric pressure and then returned back to a vacuum. This pressure cycle was repeated twice in 15 min intervals, and then the sample was left under vacuum for the remaining methanol to evaporate and allow for crystallization of Tween 80 in the lumen of the HNT.[16,41]

**2.3. Metal−Phenolic Network (MPN) Coating of Tween 80 Loaded Halloysite Nanotubes (MPN−Tween−HNT System).** 200 mg of tannic acid was added to 2 mL of methanol in a vial and sonicated in a batch sonicator for 2 min. The resulting tannic acid solution was then added to 500 mg of the Tween 80 loaded HNTs in a round-bottom flask and placed in the rotary evaporator under vacuum to allow for solvent evaporation of methanol and adsorption of tannic acid onto the HNT surface and into the ends of the lumen. The samples were then recovered and further dried for 12 h in a vacuum oven at room temperature.

The MPN stoppering of Tween 80 loaded HNT was performed by the incipient wetness procedure. Typically, 100 mg of Tween 80 loaded, tannic acid coated HNTs were spread out on a clean filter paper. A freshly prepared 24 mM solution of iron chloride hexahydrate ($FeCl_3{\cdot}6H_2O$) was added in drops over the particles, and care was ensured that all HNTs on the filter paper were contacted by the iron chloride solution to initiate the formation of the MPN complex. The pH was adjusted to 7.0 by addition of drops of a pH 7 buffer solution to ensure transition into the more stable tris-complex state of the MPN film complex.[27] The resulting sample was put in a vial and dried under vacuum (Fischer Scientific vacuum oven model 280) at 40 °C.

**2.4. Emulsion Preparation and Characterization.** The halloysite nanotubes were placed in a vial and uniformly dispersed in deionized water by using a bath sonicator (VWR B2500A) for 2 min. The ratio of HNT samples to water was kept constant at 0.5 wt %. *n*-Dodecane was then added to the HNT dispersion in the vial. The resulting ratio of dodecane to water in the vial was 1:3 by volume, which is equivalent to 25 wt % *n*-dodecane in water. Emulsions were then obtained after vortex mixing at 3000 rpm (Thermolyne Max Mix II) for 3 min. Small aliquots of the dodecane-in-water emulsion were removed using a plastic dropper pipet and imaged under a Nikon eclipse LV100 optical microscope. The images obtained were analyzed using the ImageJ v.1.52b software to evaluate the droplet size distributions.

**2.5. Thermogravimetric Analysis (TGA).** TGA of the samples was performed on a TA Instruments Q500 thermogravimetric analyzer. 20 mg of sample was placed in a 100 μL platinum pan and placed on the TGA sample tray for analysis. The analysis was performed at a heating rate of 5 °C/min in an air environment. The scanning range was 25−720 °C. The Tween 80 loading was expressed in terms of the mass percentage of Tween 80 in the Tween 80 loaded samples.

**2.6. Scanning Electron Microscopy (SEM) and Transmission Electron Microscopy (TEM).** Pristine HNTs, Tween 80 loaded HNTs, and Tween loaded HNTs that are stoppered with MPNs (MPN-Tween-HNT) were characterized by scanning electron microscopy (SEM) on a Hitachi S-4800 Field emission scanning electron microscope operated at 3 kV at a 3 mm working distance. The samples were placed on an aluminum sample holder and then sputter-coated with a thin layer of conductive carbon to dissipate charging artifacts and any resultant heat buildup during imaging. Transmission electron microscopy (TEM) was also performed by using a FEI G2 F30 Tecnai transmission electron microscope operated at 300 kV. An ∼1 mg sample was placed in a vial containing 1 mL of ethanol. After light shaking, a drop of the suspension was extracted and placed on a Formvar coated carbon 200 mesh copper grids for TEM imaging. For cut-section TEM imaging of the bare, Tween-HNT, and MPN-Tween-HNT, small fragments of the samples were impregnated with Spurr resin in a 2 mL Eppendorf tube. The tubes containing the samples were then placed in an oven for 3 days at


DOI: 10.1021/acsanm.9b00469
ACS Appl. Nano Mater. 2019, 2, 3490−3500

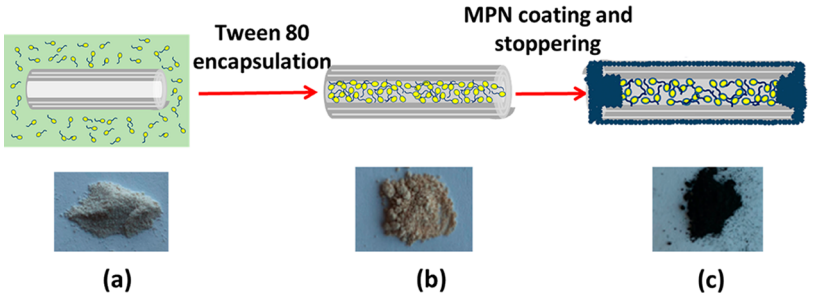


**Figure 2.** Schematic for the synthesis of MPN stoppered Tween 80 loaded. The first step is encapsulation of Tween 80 into the lumen of the HNTs by vacuum infiltration and solvent evaporation. The second step is the tannic acid infiltration by the same method followed by MPN formation by addition of iron(III) chloride via incipient wetness. Photographs are of (a) pristine HNTs (whitish powder), (b) halloysites loaded with Tween 80 (yellowish in color), and (c) halloysites that are loaded with Tween 80 and stoppered with metal–phenolic network (deep blue hue).

60 °C, then cut with a Reichelrt ultramicrotome, and then placed on TEM copper grids for imaging.

**2.7. Cryo-Scanning Electron Microscopy (Cryo-SEM).** The surface morphology of the oil–water interfacial area of the emulsions was imaged by cryo-scanning electron microscopy (Cryo-SEM). The emulsion samples for imaging were cryo-fixed by first immersing the emulsion into liquid nitrogen. The frozen samples were then fractured by striking them with a cold knife at −130 °C. The revealed fracture plane was sublimed at −85 °C in a vacuum SEM chamber for 10 min. The difference in sublimation rates of the frozen oil and water enhanced the surface topology. The sample was placed on a cryo-stage and imaged using a Hitachi S-4800 field emission scanning electron microscope under an accelerating voltage of 3 kV.

**2.8. Fourier Transform Infrared (FTIR) Spectroscopy, Energy-Dispersive X-ray Spectroscopy (EDS), and Zeta-Potential Measurements.** FTIR spectroscopy using KBr pellets of pristine, Tween 80 loaded, and Tween loaded HNTs that are stoppered with MPNs (MPN–Tween–HNT) was performed using a Thermo Nicolet Nexus 670 FTIR spectrometer. All samples for the FTIR were predried at 45 °C prior to analysis. EDS was performed on a Hitachi S-4700 scanning electron microscope operating at 15 kV and at a working distance of 10 mm. The samples to be analyzed were placed on a copper grid, and EDS spectrum was obtained and analyzed with the Oxford INCA software. The zeta-potential of each of the samples was measured using the Nanobrook ZetaPALS (Brookhaven Instruments). Typically, about 2.5 mL of the HNT dispersion in deionized water was placed in a disposable plastic cuvette cell and inserted into the cuvette holder for zeta-potential measurements.

**2.9. Interfacial Tension and Contact Angle Measurement.** The dynamic interfacial tension measurements of Tween 80 loaded HNT (without MPNs) and MPN–Tween–HNT dispersions in saline water and saline water with pH values adjusted to 2.0 and 9.0, respectively, were performed using the inverted pendant drop method on a standard Ramé-Hart model 250 goniometer. The samples were prewashed twice to remove much of the adsorbed Tween 80. About 10 mg of the washed samples was weighed into 6 mL of saline water in a glass cell. About 15 μL of dodecane was quickly injected from an inverted gauge needle into the aqueous dispersion. The shape of the drop was analyzed for about 800 s using the DROPimage Advanced software to calculate the oil–water interfacial tensions. For measurement of the three-phase water contact angles at the HNT–water–dodecane interface, the samples were first pressed into a tablet using a hydraulic lab press and placed in a glass cell containing dodecane as the external phase.[42−44] A drop of water (25 μL) was then injected from a gauge needle connected to a pump onto the surface of the HNT sample for measurement of the contact angle using the goniometer.

**2.10. Characterization of Surfactant Tween 80 Release Kinetics.** 50 mg of MPN–Tween–HNT each was placed in two Eppendorf tubes. 1 mL of saline water was added to each tube. The amount of Tween 80 loaded on the HNTs from thermogravimetric analysis (TGA) was 16.3%. The pH in each tube was adjusted to 2.0 and 9.0 by using 20 μL buffer solutions with pH values of 2.0 and 9.0, respectively. The tubes were placed on a benchtop shaker and gently agitated. Samples (100 μL) were taken at regular time intervals and were analyzed for Tween 80 release. 100 μL of saline water at the pH values in the tubes (2.0 or 9.0) was added back into the tubes after sampling to replace the withdrawn samples. The amount of Tween 80 released into the saline water was characterized by ultraviolet (UV) spectroscopy by using the cobalt thiocyanate active substances (CTAS) method.[45,46] This CTAS reagent was prepared by dissolving 20 g of $NH_4SCN$ and 3 g of $Co(NO_3)_2$ in 100 mL of deionized water. 100 μL of the samples withdrawn was diluted with 650 μL of saline water in a 7.4 mL (2 dram) vial. 750 μL of the CTAS reagent was added to the vial and briefly vortexed. Finally, 3.0 mL of chloroform ($CHCl_3$) was added to the samples followed by vortex mixing at 3000 rpm for 2 min. By use of the UV spectrometer (Shimadzu UV-1700 PharmaSpec), the absorbance of the cobalt thiocyanate–polyethoxylate complex extracted into the chloroform phase was measured at 620 nm. The concentrations of Tween 80 were evaluated from calibration curves obtained from known concentrations of Tween 80 in saline–water. As a control, the release kinetics of same amounts (50 mg) of Tween 80 loaded HNTs (without MPNs) were also characterized by using this same procedure.

## 3. RESULTS AND DISCUSSION

**3.1. Particle Characterization.** Figure 2 illustrates the synthesis of the halloysite nanotubes (HNT) that contain Tween 80 and are stoppered with metal–phenolic networks. Figure 2a illustrates the pristine HNT nanotubes that appear as a whitish powder. The first step is to encapsulate Tween 80 in the lumen which is done through the vacuum infiltration method described in the Materials and Methods section. Figure 2b shows that the powder takes on a slightly yellow color through adsorption of Tween 80 on the external surface of the HNTs. The second step is the infiltration of tannic acid and the formation of the network after addition of $FeCl_3$. When this is done, the powder assumes a deep blue hue representative of the MPN that has formed both within the lumen and on the surface of the halloysite due to iron coordination with tannic acid adsorbed on the external surface (Figure 2c).

For conciseness, detailed characterizations of the loaded halloysites using FTIR and TGA are described in the Supporting Information. Section S2 describes the FTIR spectra indicating the presence of Tween 80 through the vibrational bands attributed to the alkyl groups and the presence of MPNs through the aromatic groups in the FTIR spectrum. The TGA results (Supporting Information S3) indicate a loading of 16.3% Tween and a loading of 12.7 wt % MPNs, with the theoretical lumen loading of 14.3% assuming a lumen diameter



DOI: 10.1021/acsanm.9b00469
ACS Appl. Nano Mater. 2019, 2, 3490−3500

of 35 nm and the remainder being Tween 80 simply adsorbed on HNT. TGA analysis was performed on unwashed samples, thus leaving excess Tween 80 on the surface of the HNTs. Ideally, washed samples would be preferable to obtain the Tween loading within the lumen of HNT and also the MPN loading level. However, Tween loading levels are obtained through the subtraction of the MPN−Tween−HNT weight loss from the MPN−HNT weight loss. But fabricating MPN−HNTs in the absence of Tween will lead to MPN incorporation in the lumen, leading to inaccuracy in the Tween loading determination. Similarly, if we wash the Tween−HNT system, we will lose all the Tween 80 (as confirmed through TEM images in the Supporting Information sections S7 and S8). It is for this reason we have used the unwashed samples. Thus, the Tween−HNT versus the control of just pristine HNT gives us the total amount of Tween (both encapsulated and adsorbed). The MPN−Tween−HNT versus Tween−HNT gives us the level of MPNs. Energy-dispersive X-ray spectroscopy (EDS) measurements of the MPN−Tween−HNT system show the presence of Fe (Supporting Information S4a) while zeta-potential measurements indicate a reduction of zeta-potential from −27 ± 2 mV for native HNT to −53 ± 3 mV for the MPN coated system at pH 7 (Supporting Information S4b), perhaps indicative of an increase in anionic surface hydroxyl groups and the carboxyl acid groups. While the zeta-potential for pristine HNT is in accordance with literature values,[47,48] the reduction upon MPN coating to −53 mV is counterintuitive. In the MPN coated HNT the stoppering may inhibit mobility contributions from the cationic lumen which may additionally contribute to the observed negative zeta potential of −53 mV.

Morphological characterizations of the MPN−Tween−HNT systems are shown through the SEM images of Figure 3. Figure 3a reveals the relatively smooth surface morphology of pristine HNTs with a negligible difference in morphology seen upon Tween loading. No obvious difference in morphology is observed in the Tween 80 loaded HNTs (Figure 3b). The MPN−Tween−HNT system shown in Figure 3c shows a small increase in thickness (red arrows in Figure 3c) from 62 ± 2 nm (using ImageJ analysis) in pristine HNT to 85 ± 13 nm in the MPN coated HNT. We also see the presence of bundles of HNT held together by the MPNs (yellow arrows in Figure 3c) with bundle diameter up to 400 nm. Figure 3d illustrates the high-resolution image of one of the larger bundles with an effective bundle diameter of ∼500 nm.

Figure 4 shows the TEM images of pristine HNTs, Tween 80 loaded HNTs (Tween−HNT), and the MPN−Tween−HNT system. Figures 4a illustrates the hollow nanotubular structure of pristine HNTS with the inset focusing on a single nanotube. Figure 4b shows the Tween−HNT system where we observe a loss of clarity of the lumen since it is now loaded with Tween. Figure 4c shows the MPN−Tween−HNT system. The immediate observation is the bundling of tubes with tube aggregates that have a wide range of diameters typically 100−200 nm. A second observation is a matchstick tip type morphology on some of the HNT ends. We also note that the background contains small dark specks which are MPNs that have not attached to the HNTs. Cut-section TEM imaging of pristine HNT, Tween−HNT, and MPN−Tween−HNT (Supporting Information S5) shows some evidence of a clear lumen in the pristine HNTs and a disappearance of the lumen in Tween−HNT and MPN−Tween−HNT samples To

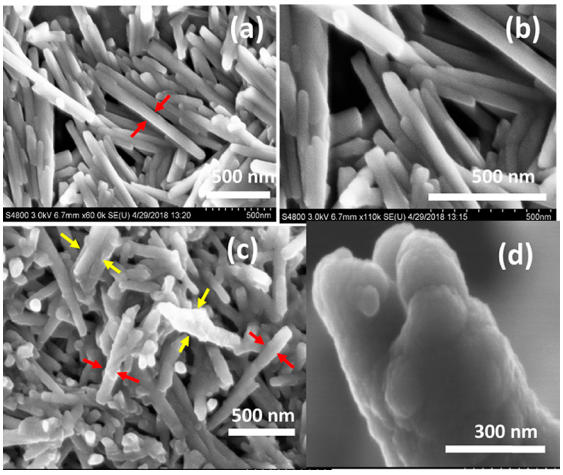


**Figure 3.** Representative electron micrographs of the halloysites. (a) SEM image of pristine halloysites showing smooth surface morphology and cylindrical nature. (b) SEM image of Tween 80 loaded HNTs. No visible difference in morphology is observed when compared to the pristine HNTs. (c) SEM image of the MPN−Tween−HNT. Yellow arrows indicate the presence of HNTs bundled up by MPNs. Red arrows show increase in thickness of HNTs when compared with pristine HNTs as measured by using ImageJ analysis software. A rougher surface morphology and increase in thickness indicate the MPN stoppering and coating of the HNTs. (d) A high-resolution SEM image showing Tween loaded HNTs bundled up by MPNs.

summarize, there is clear evidence of MPNs attaching to the Tween loaded HNT tubes to coat and bundle tubes. The stoppering aspect of MPNs can only be verified through Tween release studies which we describe in subsequent sections of the paper.

**3.2. Interfacial Characteristics.** HNTs are efficient in forming particle stabilized emulsions, also known as Pickering emulsions[14,15] with the nanotube cylindrical surfaces along the oil−water interface. In such a configuration, the particles are extremely stable at the oil−water interface, with the free energy required to remove the particle from the interface expressed as[15]

$$\Delta G_w = 2rL\gamma_{ow}\left[\sin\theta - \theta\cos\theta\left(1 + \frac{r}{L}\right) + \frac{r\cos^2\theta\sin\theta}{L}\right] \quad (1)$$

where $r$ is the cylinder radius, $\theta$ is the three-phase equilibrium contact angle, $\gamma_{ow}$ is the oil−water interfacial tension, and $L$ is the cylinder length. Figure 5a illustrates the dodecane−water contact angles of pristine HNTs and the MPN−Tween−HNT system. The three-phase contact angle for pristine HNTs is 32 ± 3° (Figure 5a(i)) indicative of a hydrophilic surface, with the free energy of detachment $\Delta G_w/kT$ value calculated as $1.82 \times 10^7$ for 1 $\mu$m HNT tubes with a diameter of 62 nm. Coating the HNT with MPNs reduces the hydrophilicity with a measured contact angle of 78 ± 3° (Figure 5a(ii)), approaching the optimal value of 90°. The increase in contact angle is perhaps counterintuitive with the coating of polyphenol-containing MPNs. Our contact angles measurements were done to mimic HNTs at an oil−water interface. We therefore made a coating of HNTs on a substrate exposed it to a bulk phase of dodecane and then placed a water droplet so that there would be a three-phase contact between HNT, water, and oil. Experiments with HNT coated with MPNs showed an increase in contact angle in comparison to just


DOI: 10.1021/acsanm.9b00469
ACS Appl. Nano Mater. 2019, 2, 3490−3500

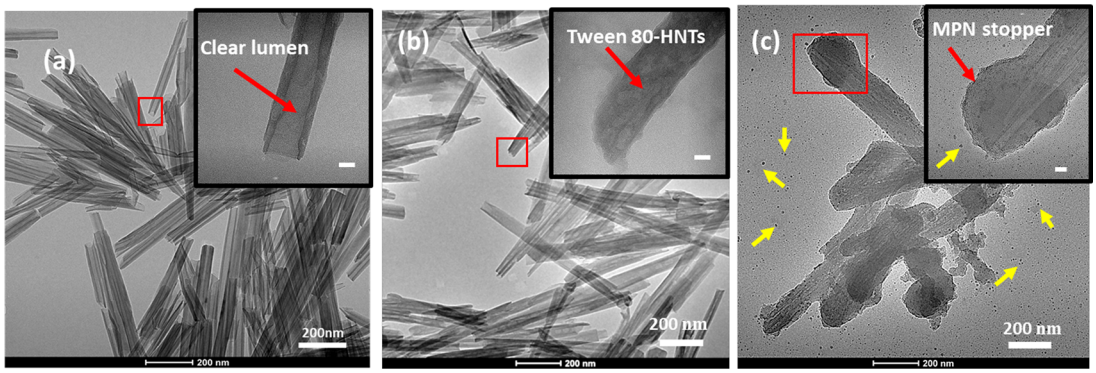


**Figure 4.** (a) TEM image of pristine halloysites showing their smooth outer and inner morphology and cylindrical nature. The inset shows the high-resolution TEM image of a pristine HNT revealing the clear lumen. (b) TEM image of Tween 80 loaded HNTs. The inset shows high-resolution TEM image of a Tween 80 loaded HNT showing the disappearance of the clear lumen. (c) TEM image of MPN−Tween−HNTs. Yellow arrows indicate surrounding MPN films not attached to HNT surface. The inset shows the high-resolution TEM image of a MPN−Tween 80−HNT system. Bundling of Tween 80 loaded HNTs by the MPNs and the presence of thin MPN films on the surface of the halloysites are also observed, in addition to the stoppers at the HNT ends. Scale bars are 200 nm. Inset scale bars are 20 nm.

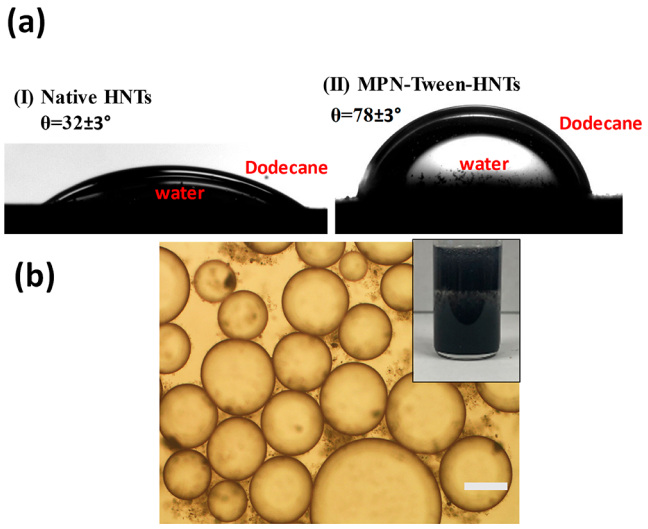


**Figure 5.** (a) Photographs showing the contact angle of water drops on (I) pristine HNT surfaces and (II) MPN−Tween−HNT surfaces in an external dodecane phase. (b) Optical microscopy images of dodecane-in-water emulsions showing the interfacial activity of MPN−Tween−HNT. HNT concentration 0.5 wt % in water. Dodecane:water ratio was 1:3 by volume. The inset is a photograph of the vial containing the emulsions. Scale bars = 100 $\mu$m.

HNT. A control experiment with MPNs on a glass substrate also showed an increase in contact angle when compared to just the glass substrate. A possibility is that oil adsorption on the polyphenol complexes of the MPN could make the MPN film more hydrophobic and thus increase the contact angle. A rough calculation of $\Delta G_w/KT$ assuming cylindrical geometry but with a coated bundle of nanotubes with diameter 200 nm yields a value of $1.52 \times 10^8$, indicating an extremely strong affinity for the interface. Emulsion droplet size distributions of the MPN−Tween−HNT system were measured by using optical microscopy (Figure 5b) and ImageJ analysis to reveal droplets of size 182.9 ± 14 $\mu$m. The emulsion stays stable for extended periods with a virtually unchanged droplet size distribution for 2 weeks. The inset to Figure 5b shows the emulsion phase with the characteristic deep blue hue of the MPNs. The subphase (water) contains some free dispersed MPNs.

Detailed imaging of the oil−water interface covered with the MPN−Tween−HNT system is shown through the cryogenic scanning electron micrographs of Figure 6. The side-on alignment of the nanotubes at the oil−water interface is clearly visible as a dense network at the oil−water interface that provides a steric hindrance to drop coalescence. Figures 6a−d show the interface at increasing resolutions from an entire droplet (Figure 6a) to a tube network with tubes and tube bundles appearing to lie somewhat parallel to each other. Supporting Information section (S6) contains images of emulsions stabilized with pristine HNTs with similar observations regarding network formation at the oil−water interface. Figures 6e,f show an interesting feature of the Cryo-SEM that we observed at the cut section of the oil−water interface. Because of the different coefficients of thermal expansion ($\alpha$) of oil and water, the vitrification produces a small gap between vitrified water and oil. We clearly see a concentration of nanotubes (or tube bundles) at the edge of this gap but on the water side. This is further evidence of HNT attachment to the oil−water interface with an alignment parallel to the interface.

**3.3. Stimuli-Responsive Release of Tween from MPN−Tween−HNT.** MPN films are pH-responsive, being stable at neutral and basic pH values and undergoing disassembly at acidic pH values[27] through protonation of hydroxyl groups which breaks the metal coordination. Figure 7a illustrates the dynamics of the oil−water interfacial tension at two pH values as a measure of the rate of release of Tween at pH 9 and pH 2 as measured by inverted pendant drop tensiometry. In these experiments, the samples were prewashed twice to remove much of the adsorbed Tween 80. While the dodecane−saline water interfacial tension is 51 mN/m, the small amount of remnant Tween on the surface MPN−Tween−HNT reduces the initial interfacial tension to ∼34 mN/m. The MPN−Tween−HNT system at a pH of 9.0 shows no significant reduction in interfacial tension indicating the stability of the MPN stoppers.

On the other hand, at pH 2, the MPN stoppers disassemble, and there is a fairly rapid release of Tween with a pseudo-first-order initial rate constant of 0.003 $s^{-1}$. We note that when the interfacial tension reaches values of ∼16 mN/m (in 1400 s), the drop detaches from the tip of the needle in the goniometer. Figure 7 also shows the extremely rapid release from HNT


DOI: 10.1021/acsanm.9b00469
ACS Appl. Nano Mater. 2019, 2, 3490−3500

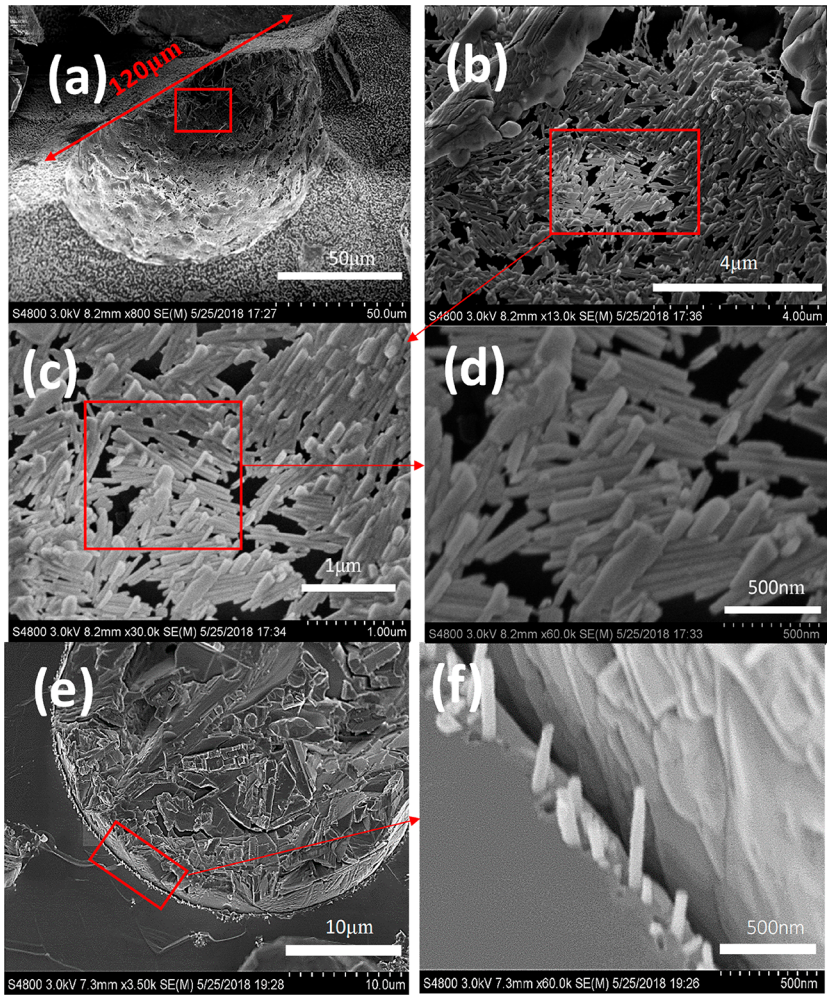


**Figure 6.** (a) Cryo-SEM image of a dodecane-in-water emulsion droplet stabilized by 0.5 wt % MPN−Tween−HNT. The average droplet size observed was 182 ± 14 $\mu$m (standard deviation). (b−d) High-resolution Cryo-SEM images of dodecane-in-water emulsion stabilized by 0.5 wt % MPN−Tween−HNT showing the dense network of halloysite nanotubes trapped at the oil−water interface. The emulsion is stabilized by the adsorption of halloysite nanotubes network at the oil−water interface. (e) Low-magnification Cryo-SEM image showing the interfacial activity of these MPN−Tween−HNT. The HNTs are seen to preferentially adsorb to the oil−water interface and not in the surrounding bulk aqueous phase. (f) High-resolution Cryo-SEM image showing the MPN−Tween−HNT protruding through the vitrified aqueous phase.

containing Tween but without an MPN stopper. The experiment was done by placing the Tween loaded HNT into the reservoir of the goniometer and immediately generating a drop at the tip. The rate of interfacial tension reduction is extremely rapid as Tween diffuses out of the HNTs with a measured initial rate constant of 0.01 $s^{-1}$ Again, the drop detaches from the tip of the needle when the interfacial tension reaches values of ∼16 mN/m. It is important to note that Tween 80 (Supporting Information section S1b) is a nonionic surfactant with a hydrophilic−lipophilic balance (HLB) value of 15.0. It is highly soluble in water, and we do not expect the surfactant to be strongly adsorbed to the halloysite through electrostatic interactions. In a saline environment representative of the marine environment (0.6 M NaCl) the Debye length is 0.4 nm, and electrostatics play an insignificant role. Release of Tween is only through diffusion driven by a concentration gradient since the diameter of the lumen (∼30 nm) is so much larger than the radius of gyration of a Tween molecule (1.06 nm).[49]

The results shown in Figure 7a are an indication of the ability of MPNs to stopper Tween release from HNT. Direct evidence of the rates of Tween 80 release is shown in Figure 7b. In these experiments described in Figure 7b, the MPN−Tween−HNT system was not washed after Tween loading and MPN stoppering to compare all systems starting from approximately the same Tween loading. Hence, the initial burst release observed in all cases is due to Tween 80 adsorbed to the exposed surfaces. The Tween 80 loaded HNTs (without stoppers) shown in case I releases all of its cargo in less than an hour consistent with results by Owoseni and co-workers.[14] A slower release of Tween at a pH of 2.0 over 12 h (case II) was observed due to the gradual disassembly of the MPN stoppers at low pH and the opening up of the HNT lumen to allow Tween 80 release into the aqueous phase. The pH 2 level is purely a laboratory experiment for convenience in showing that the MPNs can be degraded rapidly. Slower degradation can be effected at slightly acidic conditions, and even at neutral conditions, the MPNs very slowly degrade.[27] As shown in Figure 7b, the MPN−Tween−HNT at a pH of 9.0 showed a very slow rate of Tween 80 release after the initial burst for extended time periods (case III). To verify that there is Tween in the lumen, we dropped the pH to 2 after 48 h to disassemble the MPNs. This leads to a rapid release of Tween to the final levels observed cases I and II. We note that during the 48 h of



DOI: 10.1021/acsanm.9b00469
ACS Appl. Nano Mater. 2019, 2, 3490−3500

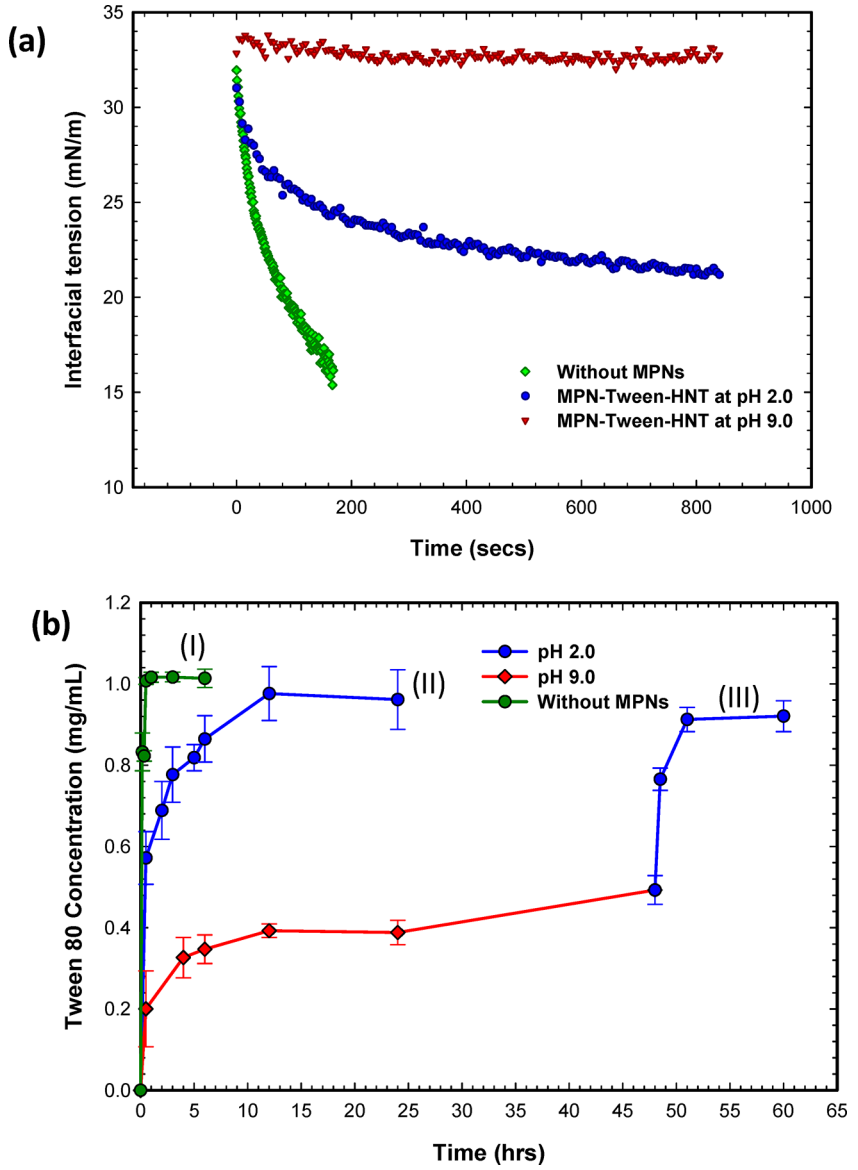


**Figure 7.** (a) Interfacial tension of the dodecane−saline water interface for MPN−Tween−HNT (16.3 wt % Tween 80) at pH of 2.0 and 9.0. Samples were washed with saline water to remove adsorbed Tween 80 prior to measurements. (b) Kinetics of surfactant release from MPN−Tween−HNT at pH of 2.0 and 9.0 (I) Tween 80 loaded HNTs without MPN stoppers. (II) MPN−Tween−HNT at pH of 2.0 (blue curve). Breakdown of MPN assembly results in gradual release of Tween 80 cargo. (III) MPN−Tween−HNT at pH of 9.0. MPN stability results in the effective sequestering of Tween 80 cargo for more than 48 h (red curve). Blue curve indicates onset of pH drop to 2.0 and subsequent Tween 80 release due to MPN disassembly.

incubation at pH 9 there could be a slow degradation of the MPNs, and subsequently when the pH is dropped to 2, there is a rapid degradation, resulting in a strong release of Tween over an hour. On the basis of TGA analysis of initial Tween loading, we note that the final amount of Tween released is ∼75% of the initial loading. Heating the samples to 60 °C to release remnant adsorbed Tween results in another 17% recovery, closing the material balance to 92% of the initial loading. We assume that the small discrepancy remaining in the material balance is due to loss of Tween during the sampling process.

Figure 8 illustrates that release can be controlled not just by using a drop in pH but additionally by adjusting the level of MPN used. The initial burst seen in Figure 8 is again due to Tween 80 simply adsorbed on the external surface of the HNT. As the MPN level is reduced from the level required to completely stopper the HNT at near neutral pH (full MPN level in Figure 8), we see that the stopper effect diminishes with the decrease in MPN level. This serves as an alternative method to control release.

Finally, Figure 9 illustrates the emulsion characteristics after MPN disassembly. Figure 9a shows the optical micrograph of the emulsion after MPN disassembly and Tween release showing a dramatic reduction in droplet size with all droplets being significantly smaller than 100 $\mu$m and small enough to be fully sustained in the water phase for extended periods. The droplet size and attendant increase in interfacial area are correlated to the interfacial tension through $\Delta G = \gamma_{ow}\Delta A$, where $\Delta G$ is the work (energy) input, $\Delta A$ is the change in interfacial area, and $\gamma_{ow}$ is interfacial tension. For the same energy input or work level (for example, the energy of breaking waves or the turbulence in a deep sea release), the interfacial area increase is inversely proportional to the interfacial tension.



DOI: 10.1021/acsanm.9b00469
ACS Appl. Nano Mater. 2019, 2, 3490−3500

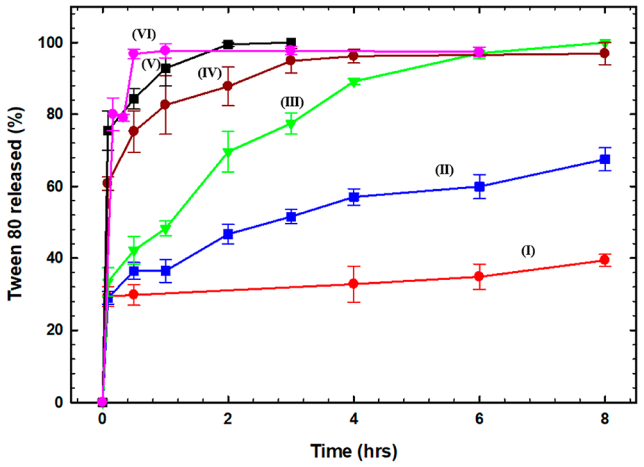


**Figure 8.** Tween 80 release kinetics of MPN−Tween−HNT obtained by tuning the levels of MPNs used: (I) full MPN level (0.4 g of tannic acid/g of halloysite), (II) 3/4 MPN level, (III) 1/2 MPN level, (IV) 1/4 MPN level, (V) 1/8 MPN level, and (VI) Tween loaded HNTs without MPN.

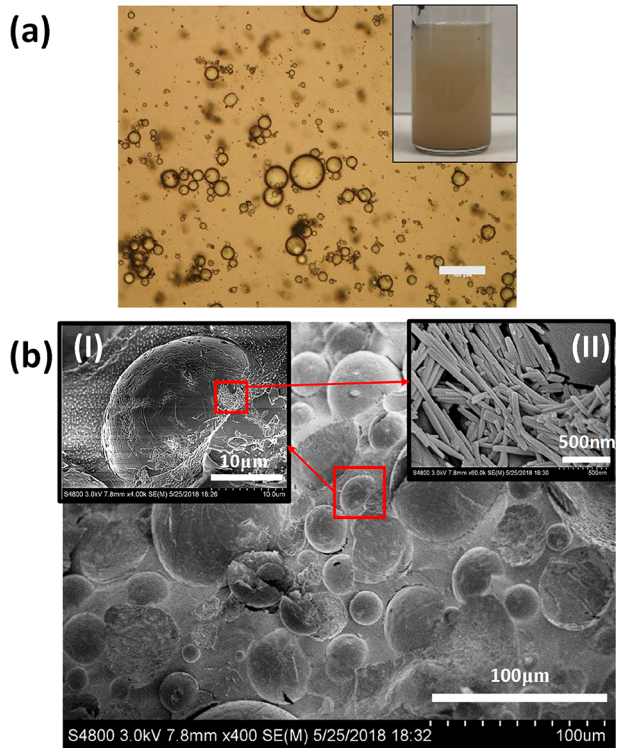


**Figure 9.** (a) MPN−Tween−HNT emulsions after disassembly of MPNs at pH of 2.0. The inset is a photograph of the vial containing the emulsions. The scale bar is 100 $\mu$m. (b) Low-magnification Cryo-SEM image of dodecane-in-water emulsion stabilized by 0.5 wt % MPN−Tween−HNTs after MPN disassembly and Tween 80 release at pH 2.0. Inset (I) is a higher resolution cryo-SEM image of an emulsion droplet. Inset (II) is the high-resolution cryo-SEM image of inset (I) showing HNTs as an unstructured network.

The use of surfactants to reduce the interfacial tension hence results in an increase in interfacial area (smaller droplets observed). Figure 9b shows the cryo-SEM images of the O/W emulsions obtained after disassembly and release of Tween 80 at a pH of 2.0, indicating the significantly reduced particle size of the droplets. The insets show a much looser network of HNT at the interface, and inset (ii) shows that the HNT morphology is unbundled and the distinct nanotubes have a smooth external morphology, indicating removal of all MPNs. The particles after the release experiments were recovered, and TEM imaging was carried out. The TEM images of MPN−Tween−HNT samples after the release of Tween 80 cargo (Supporting Information sections S7 and S8) show a clear lumen indicative of release of encapsulated cargo.

## 4. CONCLUSIONS

This work describes a new method for the targeted delivery of surfactants to the oil−water interface. The technique involves the coupling of the use of particles to stabilize oil-in-water emulsion droplets with the controlled release of surfactants encapsulated in the particles to lower the interfacial tension and generate much smaller droplets that become dispersed in the water column. The natural clay halloysite is used to stabilize oil droplets, and surfactants are encapsulated in the lumen of the nanotubes. The controlled release of surfactants from the lumen is done by using scalable and environmentally benign stoppers through the integration of metal−phenolic networks, with the gradual breakdown of the stoppers leading to a slow release of surfactant. The release can be triggered by a transient drop of pH prior to delivery or through controlling the level of the stoppering component.

The application to oil spills is as follows with the objective to effect a delayed release of surfactants at the oil−water interface so that the HNTs can stabilize the emulsion droplets against coalescence and the released surfactants can reduce the interfacial tension to low enough levels that the droplet size is sufficiently reduced to allow the droplets to be suspended in the water column. There are two methods to deliver the surfactant loaded HNTs to surface spills. In the first method, prior to delivery the granulated powder is added to water at a low pH for a short period of time. The reason for this preliminary step is to initiate the breakdown of these metal−phenolic network (MPN) stoppers, slightly opening up the lumen for the release of the surfactants. The resulting fluid is then added brought back up to neutral values and then sprayed. Spraying at neutral pH is also essential from the perspective of environmental safety. However, this process requires additional steps of modulating pH levels prior to spray delivery. The more practical way as shown through Figure 8 is to delay release by controlling the MPN levels used in stoppering the HNTs. By cutting down the level of MPNs, partial seals with thin stoppers are obtained at neutral pH values that allow a slower release. In this delivery method, the partially sealed HNTs are stored in a dry granulated form and mixed with water just prior to delivery. We note that delivery using the MPN sealed surfactant containing HNTs rather than the traditional organic solvent based dispersant formulation completely avoids the use of any solvent besides water and may be suited for light crudes where the HNTs can quickly partition to the oil−water interface.

The large, available pore volume of halloysite nanotubes for loading of different cargo coupled with the stimuli-responsive, noncytotoxic, and environmentally benign nature of the MPN stoppers have implications far beyond oil spills, in many applications requiring the controlled delivery of cargo. These applications include the controlled delivery of pharmaceuticals, pesticides, and plant nutrients and the use of surfactants in halloysite for hydraulic fracturing and controlled delivery to the


DOI: 10.1021/acsanm.9b00469
ACS Appl. Nano Mater. 2019, 2, 3490−3500

oil−water interface. Such applications are of continuing research interest in our laboratories.

## ■ ASSOCIATED CONTENT

### Supporting Information

The Supporting Information is available free of charge on the ACS Publications website at DOI: 10.1021/acsanm.9b00469.

Structures of tannic acid and Tween 80 (S1); Fourier transform infrared spectroscopy (FTIR) analysis of bare HNTs, Tween 80 loaded HNTs, and MPN−Tween−HNT (S2); thermogravimetric (TGA) analysis of bare HNTs, Tween 80 loaded HNTs, and MPN−Tween−HNT (S3); energy dispersive X-ray spectroscopy (EDS) of bare HNTs and MPN−Tween−HNT (S4a); zeta-potentials for bare HNTs and MPN−Tween−HNT (S4b); cut-section TEM images of bare HNTs, Tween−HNT and MPN−Tween−HNT (S5); Cryo-SEM images of dodecane-in-water emulsion stabilized by 0.5 wt % bare HNTs (S6); high-magnification TEM images of bare HNTs, Tween−HNT, and MPN−Tween−HNT after the release of surfactant cargo (S7); low-magnification TEM image of MPN−Tween−HNT after release of Tween 80 cargo (S8) (PDF)

## ■ AUTHOR INFORMATION


### Corresponding Author

*(V.T.J.) E-mail vj@tulane.edu.

### ORCID

Olakunle Francis Ojo: 0000-0001-9944-2148
Azeem Farinmade: 0000-0003-1343-9496
Vijay John: 0000-0001-5426-7585
Diane A. Blake: 0000-0002-7532-1541
Yuri M. Lvov: 0000-0003-0722-5643
Donghui Zhang: 0000-0003-0779-6438
Arijit Bose: 0000-0002-2309-5087


### Notes

The authors declare no competing financial interest.

The dataset can be accessed through the Gulf of Mexico Research Information and Data Cooperative (GRIIDC): https://data.gulfresearchinitiative.org (DOI: 10.7266/n7-ryhg-mp19).

## ■ ACKNOWLEDGMENTS

We gratefully acknowledge funding from the Gulf of Mexico Research Initiative, the State of Louisiana Board of Regents and Nalco-Champion Corporation. J.T. acknowledges partial support from the National Science Foundation (NSF: 1826146).

## ■ REFERENCES


(1) John, V.; Arnosti, C.; Field, J.; Kujawinski, E.; MacCormick, A. The Role of Dispersants in Oil Spill Remediation Fundamental Concepts, Rationale for Use, Fate, and Transport Issues. *Oceanography* **2016**, *29* (3), 108−117.

(2) Venkataraman, P.; Tang, J.; Frenkel, E.; McPherson, G. L.; He, J.; Raghavan, S. R.; Kolesnichenko, V.; Bose, A.; John, V. T. Attachment of a Hydrophobically Modified Biopolymer at the Oil-Water Interface in the Treatment of Oil Spills. *ACS Appl. Mater. Interfaces* **2013**, *5* (9), 3572−3580.

(3) Lessard, R. R.; Demarco, G. The significance of oil spill dispersants. *Spill Sci. Technol. Bull.* **2000**, *6* (1), 59−68.

(4) Brochu, C.; Pelletier, E.; Caron, G.; Desnoyers, J. E.; et al. Dispersion of crude oil in seawater: The role of synthetic surfactants. *Oil Chem. Pollut.* **1986**, *3*, 257−279.

(5) Allan, S. E.; Smith, B. W.; Anderson, K. A. Impact of the Deepwater Horizon Oil Spill on Bioavailable Polycyclic Aromatic Hydrocarbons in Gulf of Mexico Coastal Waters. *Environ. Sci. Technol.* **2012**, *46* (4), 2033−2039.

(6) Hemmer, M. J.; Barron, M. G.; Greene, R. M. Comparative Toxicity Of Eight Oil Dispersants, Louisiana Sweet Crude Oil (Lsc), And Chemically Dispersed Lsc To Two Aquatic Test Species. *Environ. Toxicol. Chem.* **2011**, *30* (10), 2244−2252.

(7) Athas, J. C.; Jun, K.; McCafferty, C.; Owoseni, O.; John, V. T.; Raghavan, S. R. An Effective Dispersant for Oil Spills Based on Food-Grade Amphiphiles. *Langmuir* **2014**, *30* (31), 9285−9294.

(8) Owoseni, O.; Nyankson, E.; Zhang, Y. H.; Adams, D. J.; He, J. B.; Spinu, L.; McPherson, G. L.; Bose, A.; Gupta, R. B.; John, V. T. Interfacial adsorption and surfactant release characteristics of magnetically functionalized halloysite nanotubes for responsive emulsions. *J. Colloid Interface Sci.* **2016**, *463*, 288−298.

(9) Pickering, S. Emulsions. *J. Chem. Soc., Trans.* **1907**, *91*, 2001−2021.

(10) Ramsden, W. Separation Of Solids In The Surface-Layers Of Solutions And 'Suspensions' (observations on surface membranes, bubbles, emulsions, and mechanical coagulation) Preliminary account. *Proc. R. Soc. London, Ser. A: Math., Phys. Eng. Sci.* **1903**, *72*, 156−164.

(11) Binks, B. P.; Lumsdon, S. O. Influence of particle wettability on the type and stability of surfactant-free emulsions. *Langmuir* **2000**, *16* (23), 8622−8631.

(12) Ingram, D. R.; Kotsmar, C.; Yoon, K. Y.; Shao, S.; Huh, C.; Bryant, S. L.; Milner, T. E.; Johnston, K. P. Superparamagnetic nanoclusters coated with oleic acid bilayers for stabilization of emulsions of water and oil at low concentration. *J. Colloid Interface Sci.* **2010**, *351* (1), 225−232.

(13) Katepalli, H.; John, V. T.; Bose, A. The Response of Carbon Black Stabilized Oil-in-Water Emulsions to the Addition of Surfactant Solutions. *Langmuir* **2013**, *29* (23), 6790−6797.

(14) Owoseni, O.; Nyankson, E.; Zhang, Y. H.; Adams, S. J.; He, J. B.; McPherson, G. L.; Bose, A.; Gupta, R. B.; John, V. T. Release of Surfactant Cargo from Interfacially-Active Halloysite Clay Nanotubes for Oil Spill Remediation. *Langmuir* **2014**, *30* (45), 13533−13541.

(15) Owoseni, O.; Zhang, Y. H.; Su, Y.; He, J. B.; McPherson, G. L.; Bose, A.; John, V. T. Tuning the Wettability of Halloysite Clay Nanotubes by Surface Carbonization for Optimal Emulsion Stabilization. *Langmuir* **2015**, *31* (51), 13700−13707.

(16) Panchal, A.; Swientoniewski, L. T.; Omarova, M.; Yu, T. Y.; Zhang, D. H.; Blake, D. A.; John, V.; Lvov, Y. M. Bacterial proliferation on clay nanotube Pickering emulsions for oil spill bioremediation. *Colloids Surf., B* **2018**, *164*, 27−33.

(17) Singh, B.; Mackinnon, I. D. R. Experimental transformation of kaolinite to halloysite. *Clays Clay Miner.* **1996**, *44* (6), 825−834.

(18) Vergaro, V.; Abdullayev, E.; Lvov, Y. M.; Zeitoun, A.; Cingolani, R.; Rinaldi, R.; Leporatti, S. Cytocompatibility and Uptake of Halloysite Clay Nanotubes. *Biomacromolecules* **2010**, *11* (3), 820−826.

(19) Wei, W.; Minullina, R.; Abdullayev, E.; Fakhrullin, R.; Mills, D.; Lvov, Y. Enhanced efficiency of antiseptics with sustained release from clay nanotubes. *RSC Adv.* **2014**, *4* (1), 488−494.

(20) Qi, R.; Cao, X.; Shen, M.; Guo, R.; Yu, J.; Shi, X. Biocompatibility of Electrospun Halloysite Nanotube-Doped Poly(Lactic-co-Glycolic Acid) Composite Nanofibers. *J. Biomater. Sci., Polym. Ed.* **2012**, *23* (1−4), 299−313.

(21) Liu, M.; Zhang, Y.; Wu, C.; Xiong, S.; Zhou, C. Chitosan/halloysite nanotubes bionanocomposites: Structure, mechanical properties and biocompatibility. *Int. J. Biol. Macromol.* **2012**, *51* (4), 566−575.

(22) Lvov, Y. M.; Shchukin, D. G.; Mohwald, H.; Price, R. R. Halloysite clay nanotubes for controlled release of protective agents. *ACS Nano* **2008**, *2* (5), 814−820.

(23) Abdullayev, E.; Lvov, Y. Clay nanotubes for corrosion inhibitor encapsulation: release control with end stoppers. *J. Mater. Chem.* **2010**, *20* (32), 6681−6687.
(24) Levis, S. R.; Deasy, P. B. Use of coated microtubular halloysite for the sustained release of diltiazem hydrochloride and propranolol hydrochloride. *Int. J. Pharm.* **2003**, *253* (1−2), 145−157.
(25) Nyankson, E.; Olasehinde, O.; John, V. T.; Gupta, R. B. Surfactant-Loaded Halloysite Clay Nanotube Dispersants for Crude Oil Spill Remediation. *Ind. Eng. Chem. Res.* **2015**, *54* (38), 9328−9341.
(26) Cavallaro, G.; Danilushkina, A. A.; Evtugyn, V. G.; Lazzara, G.; Milioto, S.; Parisi, F.; Rozhina, E. V.; Fakhrullin, R. F. Halloysite Nanotubes: Controlled Access and Release by Smart Gates. *Nanomaterials* **2017**, *7* (8), 199.
(27) Ejima, H.; Richardson, J. J.; Liang, K.; Best, J. P.; van Koeverden, M. P.; Such, G. K.; Cui, J.; Caruso, F. One-Step Assembly of Coordination Complexes for Versatile Film and Particle Engineering. *Science* **2013**, *341* (6142), 154−157.
(28) Betard, A.; Fischer, R. A. Metal-Organic Framework Thin Films: From Fundamentals to Applications. *Chem. Rev.* **2012**, *112* (2), 1055−1083.
(29) Ping, Y.; Guo, J.; Ejima, H.; Chen, X.; Richardson, J. J.; Sun, H.; Caruso, F. pH-Responsive Capsules Engineered from Metal-Phenolic Networks for Anticancer Drug Delivery. *Small* **2015**, *11* (17), 2032−2036.
(30) Liang, H.; Li, J.; He, Y.; Xu, W.; Liu, S.; Li, Y.; Chen, Y.; Li, B. Engineering Multifunctional Films Based on Metal-Phenolic Networks for Rational pH-Responsive Delivery and Cell Imaging. *ACS Biomater. Sci. Eng.* **2016**, *2* (3), 317−325.
(31) Kim, S.; Philippot, S.; Fontanay, S.; Duval, R. E.; Lamouroux, E.; Canilho, N.; Pasc, A. pH- and glutathione-responsive release of curcumin from mesoporous silica nanoparticles coated using tannic acid-Fe(III) complex. *RSC Adv.* **2015**, *5* (110), 90550−90558.
(32) Guo, J.; Ping, Y.; Ejima, H.; Alt, K.; Meissner, M.; Richardson, J. J.; Yan, Y.; Peter, K.; von Elverfeldt, D.; Hagemeyer, C. E.; Caruso, F. Engineering Multifunctional Capsules through the Assembly of Metal-Phenolic Networks. *Angew. Chem., Int. Ed.* **2014**, *53* (22), 5546−5551.
(33) Zeng, T.; Zhang, X.; Guo, Y.; Niu, H.; Cai, Y. Enhanced catalytic application of Au@polyphenol-metal nanocomposites synthesized by a facile and green method. *J. Mater. Chem. A* **2014**, *2* (36), 14807−14811.
(34) Wei, J.; Liang, Y.; Hu, Y. X.; Kong, B. A.; Simon, G. P.; Zhang, J.; Jiang, S. P.; Wang, H. T. A Versatile Iron-Tannin-Framework Ink Coating Strategy to Fabricate Biomass-Derived Iron Carbide/Fe-N-Carbon Catalysts for Efficient Oxygen Reduction. *Angew. Chem., Int. Ed.* **2016**, *55* (4), 1355−1359.
(35) Pasbakhsh, P.; Churchman, G. J.; Keeling, J. L. Characterisation of properties of various halloysites relevant to their use as nanotubes and microfibre fillers. *Appl. Clay Sci.* **2013**, *74*, 47−57.
(36) Lisuzzo, L.; Cavallaro, G.; Pasbakhsh, P.; Milioto, S.; Lazzara, G. Why does vacuum drive to the loading of halloysite nanotubes? The key role of water confinement. *J. Colloid Interface Sci.* **2019**, *547*, 361.
(37) Veerabadran, N. G.; Price, R. R.; Lvov, Y. M. Clay nanotubes for encapsulation and sustained release of drugs. *Nano* **2007**, *2* (2), 115−120.
(38) Qi, R. L.; Guo, R.; Shen, M. W.; Cao, X. Y.; Zhang, L. Q.; Xu, J. J.; Yu, J. Y.; Shi, X. Y. Electrospun poly(lactic-co-glycolicacid)/halloysite nanotube composite nanofibers for drug encapsulation and sustained release. *J. Mater. Chem.* **2010**, *20* (47), 10622−10629.
(39) Fan, L.; Zhang, J. P.; Wang, A. Q. In situ generation of sodium alginate/hydroxyapatite/halloysite nanotubes nanocomposite hydrogel beads as drug-controlled release matrices. *J. Mater. Chem. B* **2013**, *1* (45), 6261−6270.
(40) Rao, K. M.; Nagappan, S.; Seo, D. J.; Ha, C. S. pH sensitive halloysite-sodium hyaluronate/poly(hydroxyethyl methacrylate) nanocomposites for colon cancer drug delivery. *Appl. Clay Sci.* **2014**, *97−98*, 33−42.
(41) Ward, C. J.; Song, S.; Davis, E. W. Controlled Release of Tetracycline-HCl from Halloysite-Polymer Composite Films. *J. Nanosci. Nanotechnol.* **2010**, *10* (10), 6641−6649.
(42) Cavallaro, G.; Lazzara, G.; Milioto, S.; Parisi, F. Hydrophobically Modified Halloysite Nanotubes as Reverse Micelles for Water-in-Oil Emulsion. *Langmuir* **2015**, *31* (27), 7472−7478.
(43) Yan, N. X.; Masliyah, J. H. Effect of pH on adsorption and desorption of clay particles at oil-water interface. *J. Colloid Interface Sci.* **1996**, *181* (1), 20−27.
(44) Abdullayev, E.; Price, R.; Shchukin, D.; Lvov, Y. Halloysite Tubes as Nanocontainers for Anticorrosion Coating with Benzotriazole. *ACS Appl. Mater. Interfaces* **2009**, *1* (7), 1437−1443.
(45) Mata-Sandoval, J. C.; Karns, J.; Torrents, A. Influence of rhamnolipids and Triton X-100 on the biodegradation of three pesticides in aqueous phase and soil slurries. *J. Agric. Food Chem.* **2001**, *49* (7), 3296−3303.
(46) Crabb, N. T.; Persinger, H. E. The determination of polyoxyethylene non-ionic surfactants in water at the parts per million level. *J. Am. Oil Chem. Soc.* **1964**, *41*, 752−755.
(47) Fakhrullina, G. I.; Akhatova, F. S.; Lvov, Y. M.; Fakhrullin, R. F. Toxicity of halloysite clay nanotubes in vivo: a Caenorhabditis elegans study. *Environ. Sci.: Nano* **2015**, *2* (1), 54−59.
(48) Zhao, Y. F.; Abdullayev, E.; Vasiliev, A.; Lvov, Y. Halloysite nanotubule clay for efficient water purification. *J. Colloid Interface Sci.* **2013**, *406*, 121−129.
(49) Amani, A.; York, P.; de Waard, H.; Anwar, J. Molecular dynamics simulation of a polysorbate 80 micelle in water. *Soft Matter* **2011**, *7* (6), 2900−2908.


DOI: 10.1021/acsanm.9b00469
*ACS Appl. Nano Mater.* 2019, 2, 3490−3500